

Recovery of Electron-Irradiated Aluminum and Aluminum Alloys.

II. Stage II

K. R. GARR*

Atomics International, A Division of North American Aviation, Incorporated, Canoga Park, California

AND

A. SOSIN

North American Aviation Science Center, Thousand Oaks, California

(Received 22 May 1967)

The recovery of the residual electrical resistivities of pure Al and the Al (nominally 0.1 at.%) alloys Al-Mg, Al-Ga, and Al-Ag has been investigated following 1-MeV electron irradiation near 4°K. The addition of solute atoms caused a suppression of recovery normally observed in stage I (<70°K) for pure Al. This suppression amounted to 20–27% of the recovery of the pure sample. The stage-II (70–170°K) recovery of pure Al occurs throughout the whole temperature range. However, well-defined recovery regions were observed between 70 and 90°K and between 120 and 140°K. In the alloy system, the recovery characteristics varied with the particular solute addition. Specifically, Al-Mg showed two distinct substages of recovery in stage II, centered at 81 and 127°K. Al-Ga showed a doublet (two partially overlapping substages) centered at about 111°K. Al-Ag showed no distinct substages of recovery which could be attributed to the addition of the solute. None of the substage kinetics follow integral reaction orders when analyzed with chemical rate theory, indicating complex annealing processes.

I. INTRODUCTION

THE influence of foreign atoms on the radiation damage and recovery characteristics of nominally pure, monatomic metals has been examined with increasing interest in recent years. A number of different manifestations have been proposed and experimental evidence presented for each. In the displacement process during irradiation, impurities may be displaced with greater ease at lower transfer energies than host atoms in some cases¹; impurities may also induce further host lattice damage by defocussing of replacement sequences.² The influence of impurities on post-irradiation recovery in most fcc metals (gold being a possible exception) may be best categorized by the familiar recovery stage system. In stage I, typically below 70°K, impurities clearly interact with interstitial atoms which migrate.^{2–5} It has been generally agreed that impurity detrapping (release of interstitials from impurity traps) plays a dominant role in stage II, typically from 70 to 200°K.^{2–11} In stage III, the role of impurities is less clear.^{2,7–11} Some evidence has indicated that impurities

may play no significant role in the kinetic nature of stage III; other evidence appears to demonstrate that the role of impurity atoms may be important.

The purpose of the present paper is to examine in some depth the role of impurities in aluminum on stage II. In the following paper¹² we will discuss results on stage III. The work has consisted of two parts. In one portion, dilute alloys, containing about 0.1 at. % Mg, Ag, or Ga, were investigated; in the other portion, nominally pure samples were used. In the latter case, however, the residual electrical resistivity of the samples differed among each other, presumably indicating varying impurity content. Even these rather slight variations have proven to give rise to significantly different recovery characteristics.

A. Experimental

The cryostat used in these experiments has been described fully elsewhere by Sosin and Neely.¹³ The samples were irradiated with 1-MeV electrons to a total flux of approximately 1.8×10^{18} electrons/cm². Temperature during annealing was controlled to $\pm 0.1^\circ\text{K}$ throughout the temperature range investigated. The reproducibility of the voltage readings is of the order of 10^{-8} V, which results in an experimental uncertainty of the order of 10^{-12} Ω cm.

B. Sample Preparation

The alloys used in this work were fabricated from ALCOA 99.995% (4N5) pure Al as a base material and the appropriate amounts of magnesium, gallium,

* Work supported by Division of Research, Metallurgy and Materials Programs U. S. Atomic Energy Commission, under Contract No. AT(04-3)-701.

¹ W. Bauer and A. Sosin, *J. Appl. Phys.* **35**, 703 (1964).

² A. Sosin and L. H. Rachal, *Phys. Rev.* **130**, 2238 (1963).

³ T. H. Blewitt, R. R. Coltman, C. E. Klabunde, and T. S. Noggle, *J. Appl. Phys.* **28**, 639 (1957).

⁴ A. Sosin and H. H. Neely, *Phys. Rev.* **127**, 1465 (1962).

⁵ C. L. Snead and P. E. Shearin, *Phys. Rev.* **140**, A1781 (1965).

⁶ D. G. Martin, *Phil. Mag.* **6**, 839 (1961).

⁷ F. Dworschak and J. S. Koehler, *Phys. Rev.* **140**, A941 (1965).

⁸ D. A. Grenning and J. S. Koehler, *Phys. Rev.* **144**, 439 (1966).

⁹ S. Ceresara, T. Federighi, and F. Pieragostini, *Phys. Letters* **6**, 152 (1963).

¹⁰ S. Ceresara, T. Federighi, and F. Pieragostini, *Phil. Mag.* **10**, 893 (1964).

¹¹ W. Bauer, *Phys. Letters* **19**, 180 (1965).

¹² K. R. Garr and A. Sosin, following paper, *Phys. Rev.* **162**, 681 (1967).

¹³ A. Sosin and H. H. Neely, *Rev. Sci. Instr.* **32**, 922 (1961).

TABLE I. Concentration of solute in Al.

Sample (nominally 0.1 at. %)	Concentration as calculated by Ref. 14	Concentration according to Nock's data	Concentration as used in this report
Al-Mg	0.061	0.057	0.06 ₀
Al-Ga	0.085	0.082	0.08 ₅
Al-Ag	0.095	0.092	0.09 ₅

or silver. The silver was obtained from COMINCO. Separate tests on this material resulted in a resistivity ratio ($\rho_{RT}/\rho_{4.2^\circ\text{K}}$) of 1300. The magnesium was obtained from Johnson-Matthey and Company with a stated purity of 99.994%. The gallium was obtained from Eagle Picher and was specified as electronic grade.

Aluminum pieces, along with the appropriate amount of dopant, were placed in graphite crucibles (National Carbon Company AGKSP, spectrographic pure) and heated in vacuum (5×10^{-5} Torr) to the melting point of Al or of the solute, whichever was the higher, and held for a short time. Except for Al-Mg, which was immediately removed from the furnace and cooled (in vacuum), the ingots were allowed to furnace cool to room temperature.

After removal from the crucibles, the ingots were etched in a HCl-HF-H₂O solution. The ingots were then rolled into rods, drawn through iron wire drawing dies to a diameter of about 0.1 in. The wires were cleaned and then machined to a diameter of 0.045 in. The wires were etched once more and then drawn through a set of diamond wire drawing dies to the final diameter of 0.0021 in.

The wires were then placed on the sample holder and annealed in vacuum (1×10^{-6} Torr) for 4 h at 180°C, and furnace-cooled. This low annealing temperature was dictated by the high vapor pressure of magnesium. After annealing, the samples were soft soldered to the holder using Eutectic 1909 flux and solid 50/50 solder.

The impurity concentration of the samples was calculated from the increased residual resistivity at liquid-helium temperature according to method of Robinson and Dorn,¹⁴ and by using values obtained from ALCOA.¹⁵ The concentrations as calculated are given in Table I.

The values of the solute concentration obtained from the calculations indicate that the alloying atoms were mainly retained in solid solution. The lower value of solute concentration calculated for the Al-Mg alloy is believed to be due to loss of Mg during the initial fabrication of the alloy ingot.

Samples of Al-Cu and Al-Zn were also produced and exploratory isochronal anneals were performed on these samples using liquid hydrogen ($\sim 20^\circ\text{K}$) as the primary coolant. However, recovery of these samples from

liquid helium was not investigated in detail and, therefore, the actual solute concentration is not known accurately.

II. METHODS OF ANALYSIS

The results of the experiments described here are analyzed, unless otherwise stated, in terms of chemical rate theory. The governing equation is then taken as

$$dn/dt = -[\sigma\gamma^{-1}A\nu_0 \exp(-E/kT)]n^\gamma, \quad (1)$$

where n is the concentration of defects being monitored, E is the activation energy of the process, assumed constant, ν_0 is the atomic vibrational frequency, σ is the number of atomic sites around a reaction site in which the reaction may occur (or leading directly to reaction), and k , T , and t are Boltzmann's constant, absolute temperature, and time, respectively. The factor A takes into account entropy factors, steric factors, defect correlations, and sink or trap distributions. The order of the reaction is specified by the constant γ . In the course of analyzing the results presented below, we have investigated alternative formulations for recovery analysis. Our attempts based on the recent formulation of Nihoul and Stals¹⁶ are discussed later.

In the case of isothermal studies, Eq. (1) may be written as

$$dn/dt = -Kn^\gamma, \quad (2)$$

where all constants are incorporated into K , including the exponential temperature dependence. Integration of Eq. (2) gives the familiar results

$$\ln(n_0/n) = Kt, \quad \gamma = 1 \quad (3a)$$

$$n^{1-\gamma} - n_0^{1-\gamma} = K(\gamma-1)t, \quad \gamma > 1. \quad (3b)$$

The principal result of an isothermal study is the measurement of γ . Taking n proportional to $\Delta\rho$, the resistivity increment ($\Delta\rho = \rho_F n$, where ρ_F is the Frenkel resistivity), we write, from Eq. (3b),

$$(\Delta\rho)^{1-\gamma} = C(t+M). \quad (4)$$

To use Eq. (4), $\ln\Delta\rho$ is plotted against $\ln(t+M)$ with a selection of the adjustable parameter M until a straight line results. The slope of this line is $(1-\gamma)^{-1}$, yielding a value for γ . Even in the case of $\gamma=1$, this procedure may be used; in this case, the resulting line is vertical (has infinite slope). The procedure is valuable in that it reduces the search for γ to a systematic procedure and avoids the tendency of testing merely integral values of γ . The implication of nonintegral values of γ is discussed later, as is a discussion of the sensitivity of the method.

The value of γ obtained from Eq. (4) may be tested by further plotting $(\Delta\rho)^{1-\gamma}$ versus t , a plot which should yield a straight line for the correct value of γ . The two

¹⁴A. T. Robinson and J. E. Dorn, *J. Metals* **3**, 457 (1951); *Trans. AIME* **191**, 457 (1961).

¹⁵J. A. Nock (private communication).

¹⁶J. Nihoul and L. Stals, *Phys. Status Solidi* **17**, 295 (1966); see also R. Gevers, J. Nihoul, and L. Stals, *ibid.* **15**, 701 (1966).

TABLE II. Summary of results of stage-II annealing stages for aluminum alloys.

Sample	Temperature of stage (°K)	Isothermal temperature (°K)	Order of reaction (γ)	Activation energy E_s isochronal method (eV)	Temperature range of E_s (°K)	Activation energy E_s M-B method (eV)	Temperature range of E_s (°K)	Effective frequency factor ^a ν_e
Al 0.06 ₀ at. % Mg	81	79	1.6 ₀	0.22±0.03	76 - 86.5	0.26±0.04	79-86.5	5.6×10 ¹⁴
		80	1.6 ₀					
	127	126	1.6 ₀					
Al 0.08 ₅ at. % Ga	111	127.5	1.9 ₀	
		107.5	1.6 ₀					
		109	1.4 ₅					

^a Calculated from isochronal method of energy determination.

methods of plotting are complementary, each being most sensitive to different portions of the reaction being analyzed. In all cases reported here, both methods were used to obtain values of γ .

We now turn to isochronal studies. Recognizing that an isochronal study consists of a sequence of short isothermal anneals of equal time Δt at sequentially higher temperatures, we may write

$$\ln(\Delta\rho_{i-1}/\Delta\rho_i) = A\nu_0\Delta t \exp(-E/kT_i), \quad \gamma=1 \quad (5a)$$

$$\Delta\rho_i^{1-\gamma} - \Delta\rho_{i-1}^{1-\gamma} = A\nu_0\sigma^{\gamma-1}(\gamma-1)\Delta t\rho_i^{1-\gamma} \times \exp(-E/kT_i), \quad \gamma>1. \quad (5b)$$

Equation (5) may be used to evaluate the activation energy E assuming that the order of kinetics has been derived from a separate isothermal study via Eq. (4). The method consists of plotting the logarithms of the left-hand side versus $1/T_i$; the slope is proportional to E . In principle, this method may be made even more effective; that is, a straight line on such a plot should result only for the simultaneously correct values of γ and E . Our experience indicates, however, that the quality of fit is rather insensitive to the value of γ ; isothermal studies are to be preferred for the evaluation of γ .

As an alternative to the above method of determining activation energy, we have also used the Meechan-Brinkman method.¹⁷ In this method, two samples are required; one annealed isothermally, the other isochronally. Isothermal times and isochronal temperatures are related by the equation

$$\ln(\Delta\tau)_i = C' - E/kT_i, \quad (6)$$

where $(\Delta\tau)_i = \tau_i - \tau_{i-1}$, and τ_i is the isothermal time required to reach the value of $\Delta\rho_i$ which has been realized after the isochronal pulse at temperature T_i . C' is a constant. The indicated plot is a $\ln(\Delta\tau)_i$ -versus- $1/T_i$ graph; the slope is again proportional to E . The advantage of this method is that an explicit value of γ never enters directly into the energy analysis. Indeed, the method is very general, considerably more general than a simple chemical rate theory formulation would

indicate. However, the need for two samples poses experimental problems on occasion. When possible, we have used both methods of analysis.

It is also instructive to compare the experimental isochronal curve to one derived from chemical rate theory. This may be done by using Eq. (5). A product $A\nu_0\sigma^{\gamma-1}$ is treated as a single adjustable parameter and ρ_F is somewhat arbitrarily taken as 5×10^{-4} Ω cm/unit concentration of defects in the present work. The product $A\nu_0\sigma^{\gamma-1}$ may also be calculated from the experimental isothermal or isochronal data, once γ and E have been determined, by use of Eqs. (4) or (5). This was done for all samples whenever the data was available.

As we shall show later, our analysis based on the methods outlined in this section has met with only partial success. Further analysis based on less restrictive assumptions are presented later, along with the discussion.

III. RESULTS

Figure 1 shows the recovery pattern from 20 to 300°K for all the alloys studied here, as well as for nominally (4N5) pure aluminum. The characteristic patterns of recovery stages are apparent. In most cases, the individual stages have been experimentally analyzed in some detail. These results are collected into Table II and discussed further below. The tabulated values of energies and frequencies are denoted as effective values; the significance of this is explained later.

The prominent features discernible in Fig. 1 are: (1) suppression of stage-I (<70°K) recovery by all intentional dopants, the amount of suppression being 20-27% of the recovery present in the pure aluminum. (2) Different recovery is observed in stage II (70-170°K), depending on the solute added. Al-Mg has two stages: The first is centered at 81°K; the second, at 127°K. Al-Ga has a doublet stage, that is, two partially overlapping stages in the same temperature region, centered at about 111°K. Al-Ag has no distinct stage of recovery due to the addition of Ag atoms but shows small amounts of recovery at about 80, and about 125°K. (3) Stage-III (170-300°K) recovery for the alloys is much broader and centered at a lower

¹⁷ C. J. Meechan and J. A. Brinkman, Phys. Rev. **103**, 1193 (1956).

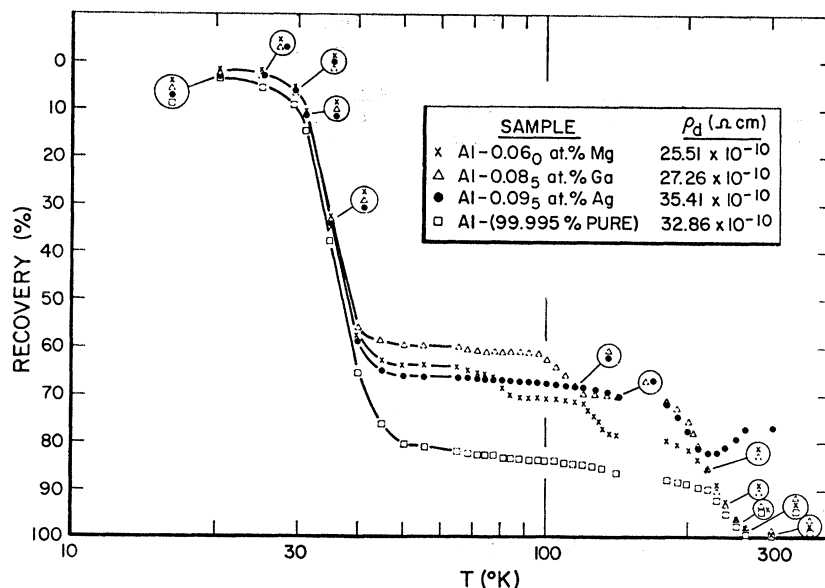


FIG. 1. The complete recovery spectrum for pure aluminum and the aluminum alloys investigated. The shape of the curve above 265°K for the Al-Ag sample was more evident in an exploratory investigation which extended to 340°K.

temperature than in pure aluminum. There is almost complete recovery in all samples, except Al-Ag, by 300°K. Al-Ag here shows a decrease in resistivity followed by an increase starting about 230°K and lasting until about 285–290°K, after which there is another decrease. This latter decrease was more evident in a previous exploratory investigation which extended to 340°K;¹⁸ stage-III results are discussed in the following paper.

A. Pure Aluminum

We now consider the details of the recovery for stage II in pure aluminum. Figure 2 pertains to aluminum of various purities as indicated by the various values of ρ_0 , the residual resistivity measured at 4.2°K (lower values of ρ_0 are presumably indicative of higher purity material). The solid curves show the results for the four samples irradiated and annealed simultaneously. The dashed line (square symbol) is for a pure Al sample which was irradiated and annealed along with alloyed samples (see Fig. 1). Recovery appears to occur throughout the whole temperature region. However, there are well-defined recovery regions: 70 to 90°K and 120 to 140°K.

Further data for the region between 70 and 90°K are shown in Fig. 3. This region has two substages of recovery, centered at 73.5 and 81.5°K. The first substage appears to be relatively insensitive to the residual impurities but does seem to increase slightly with increasing purity. The second stage, however, is seen to decrease considerably as the purity is increased. This is shown more clearly in the temperature derivative of the isochronal $d\rho_a/dT$ which is plotted in the lower portion of Fig. 3, ρ_a being the resistivity incre-

ment due to defects. The dashed segments between 82 and 84°K reflect a change in the temperature intervals used in the isochronal anneal. The observed impurity dependences appear to offer some evidence that the lower temperature substages are intrinsic in nature—that is, they are due to the recovery of defects which are either produced directly by the irradiation or during the annealing of defects in stage I with no significant effect attributable to residual impurities. The higher temperature substage appears rather to be associated with the difference in the preirradiation residual resistivity.

B. Alloys

Looking now at the recovery in stage II for the alloys, Figs. 4 and 5 show the two substages in the Al-Mg alloy. The derivative of the isochronal is shown in the bottom portion of each figure. Both of these substages appear to be singly activated stages of recovery. This was tested by a comparison of the data with calculations of the theoretical shape of the stages using Eq. (5) and the energy and kinetics data from Table II. Isothermal curves and energy determination plots for these substages are given in Figs. 6 and 7.

The order of reaction as reported in Table II for the Al-Mg IIb substage is of some concern as different values were obtained for the two isothermals reported. This variation is somewhat larger than that usually observed in such investigations. The source of variation is unknown. For this reason, the effective frequency factor is not given in Table II since a calculation of the frequency depends on the value of reaction order [see Eq. (5)]. Also, the value of γ used for the energy determination shown in Fig. 7 was 1.5 for this sample. The energy obtained using the quoted values of γ were

¹⁸ A. Sosin and K. R. Garr, *Acta Met.* **15**, 1250 (1967).

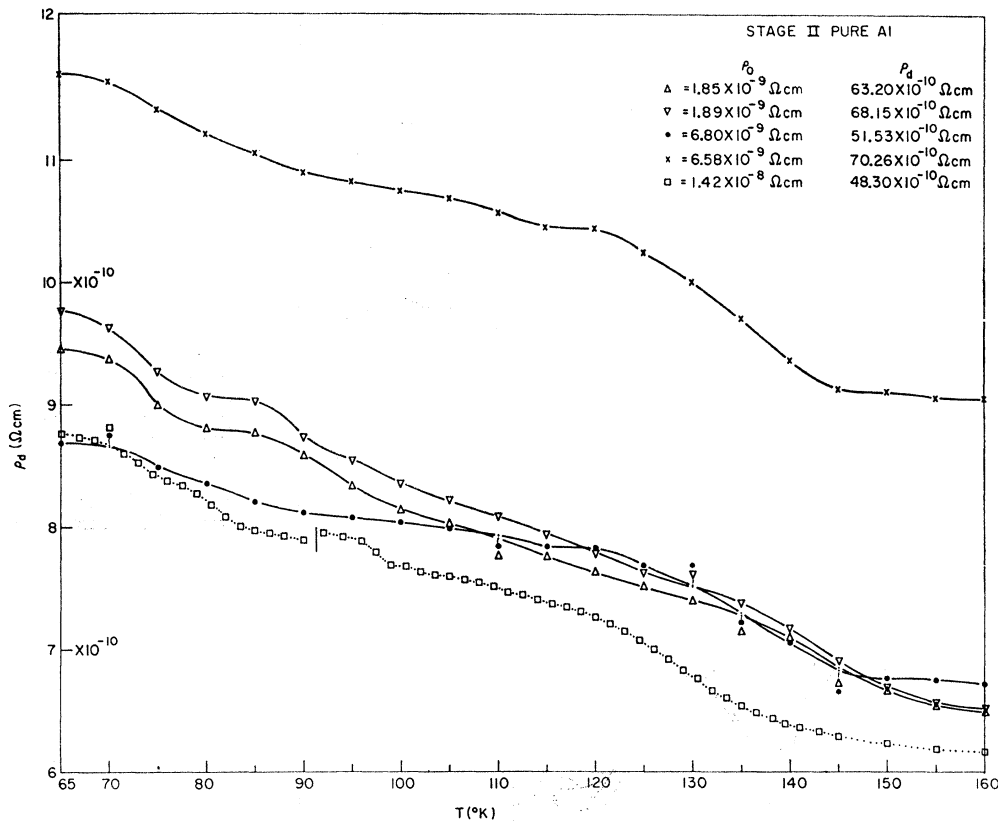


FIG. 2. Stage-II isochronal plot for Al of various purities, indicated by distinct values of the residual resistivity (ρ_0). Solid lines pertain to samples irradiated and annealed simultaneously. The dashed line (square symbol) is for the pure Al sample used with the alloys.

within the stated error but the fit of the data was not as good as that shown in Fig. 7.

The Al-Ga alloy substage (see Figs. 6-8) appears at first glance of the isochronal curve (top portion of Fig. 8) to be a single stage. However, the derivative of the isochronal (bottom portion of Fig. 8) indicates a more complex substructure. This complex substructure was verified by calculating the theoretical shape, using Eq. (5), of a uniquely activated process centered at 111°K with $\gamma=1.5$ (approximately the average value of γ obtained from the two isothermal anneals, see Table II) and an activation energy of 0.29 eV. The theoretical curve was considerably narrower in temperature range covered than the experimental curve, indicating the possibility that more than one process is active in this substage.

The value of 0.29 eV was not determined directly. Rather, it was chosen by assuming that the energy is proportional to the center temperature (i.e., the temperature at which an isochronal plot shows an inflection point). Using $T_c=111^\circ\text{K}$ in Al-Ga and the data for the nearby stage in Al-Mg where $E_a=0.33$ eV and $T_c=127^\circ\text{K}$, one obtains the above stated value for the activation energy. Fortunately, the width of the calculated curve is insensitive to the value of the activation energy.

Al-Ag showed no distinct stage of recovery in the stage-II region which can be clearly attributed to the addition of the solute. The small amount of recovery in the 120-130°K region we attribute to the residual impurities in the base material as the percentage recovery is about equal in this alloy and the pure Al sample. The results of the Al-Ag sample were verified in this work by making a new ingot of this alloy and fabricating a new sample. This was done following the exploratory isochronal anneal which revealed the unusual results in stage III shown in Fig. 1. The earlier results were confirmed in both stages II and III.

IV. DISCUSSION

A. Preliminary Remarks

Before entering into a discussion of stage-II annealing for Al and Al alloys, we summarize the results of this work. Pure Al has two small substages: at 73.5 and 81.5°K. The lower-temperature substage may be intrinsic while the higher-temperature substage is apparently associated with impurities. All dopants caused suppression of stage-I recovery normally observed in pure Al. Stage-II recovery depends on the particular solute added; specifically, Mg produces two substages between 70 and 170°K, Ga produces a

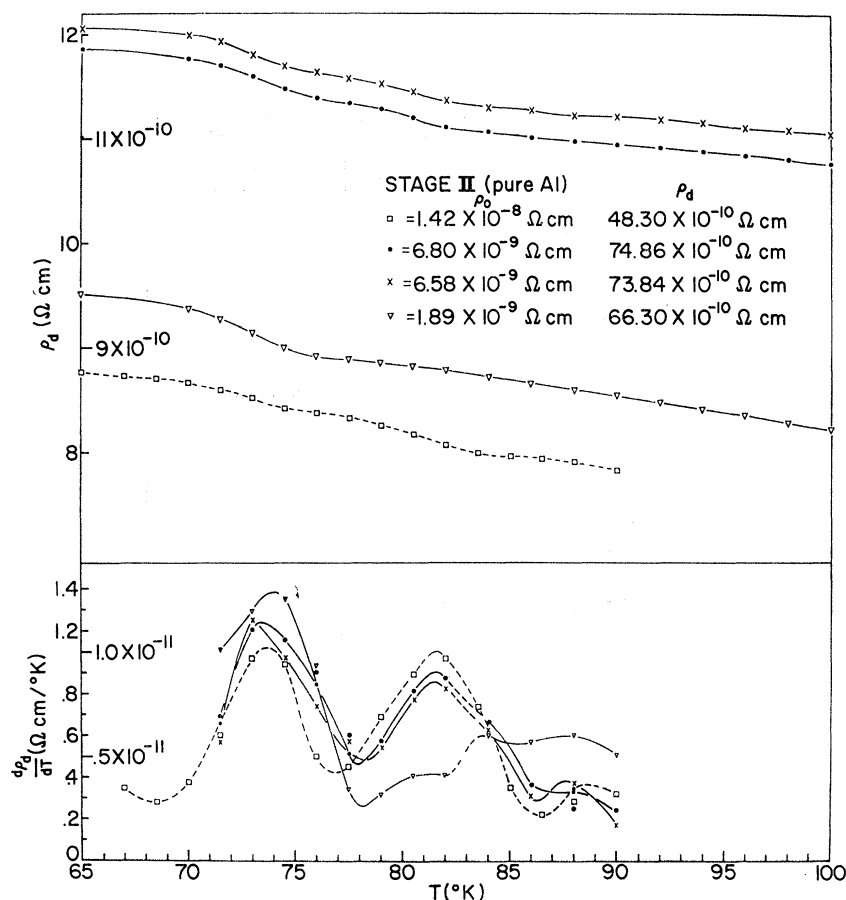


FIG. 3. Isochronal plot of stage II between 65 and 100°K for Al of various purities. Solid lines are for samples irradiated and annealed simultaneously. The dashed line (square symbol) is for the pure Al sample used with the alloys. The lower portion of the figure shows the derivative of the isochronal plot.

doublet stage, and Ag produces no distinct recovery stage. All substages observed in the stage-II region followed fractional orders of reaction, when analyzed by chemical rate theory, indicating complex annealing processes.

(Concerning fractional orders of reaction, Sosin and Rachal² reported that first-order kinetics $\gamma=1$ seemed consistent with the data for the substage observed in stage-II for the Al-0.1-at.% Zn alloy which they investigated. This was done on the strength of being able to fit the data to a reasonably straight line in the energy determination with $\gamma=1$. However, as noted earlier, this does not provide a sensitive determination of the value of the reaction coefficient used. A direct analysis of the data in that experiment yields $\gamma \approx 1.8$. Ceresara *et al.*,⁹ and Snead and Shearin⁵ did not report on the kinetics of the substages they observed; therefore, no direct comparison can be made with their work on this point.)

B. Stage II_A

Although it is generally agreed upon that stage II is due to the release of trapped interstitials, some investigators propose that other processes may be of

importance in the region between 60–100°K, the stage II_A region. Swanson¹⁹ deformed prequenched and unquenched aluminum in liquid helium and observed recovery in both cases in the temperature region from 60 to 100°K. This range is sufficiently above stage I in aluminum that they designated it as II_A. Their main observations were that II_A was enhanced by prior deformation and low-temperature annealing, suppressed by impurities, and hardly affected by prequenching. They suggested that these behaviors could best be understood by ascribing II_A to the migration of di-interstitials.

Burger *et al.*²⁰ neutron-irradiated pure aluminum. They observed a recovery peak in the 80°K region which they attributed to free interstitial migration. This assignment was made on the basis of an apparent temperature shift of the stage as the irradiation dose was increased. The possibility of detrapping was discounted by them on the grounds that their defect concentration was far in excess of the impurity concentration.

¹⁹ M. L. Swanson, *Can. J. Phys.* **42**, 1890 (1961).

²⁰ G. Burger, H. Meissner, and W. Schilling, *Phys. Statu, Solidi* **4**, 267 (1964).

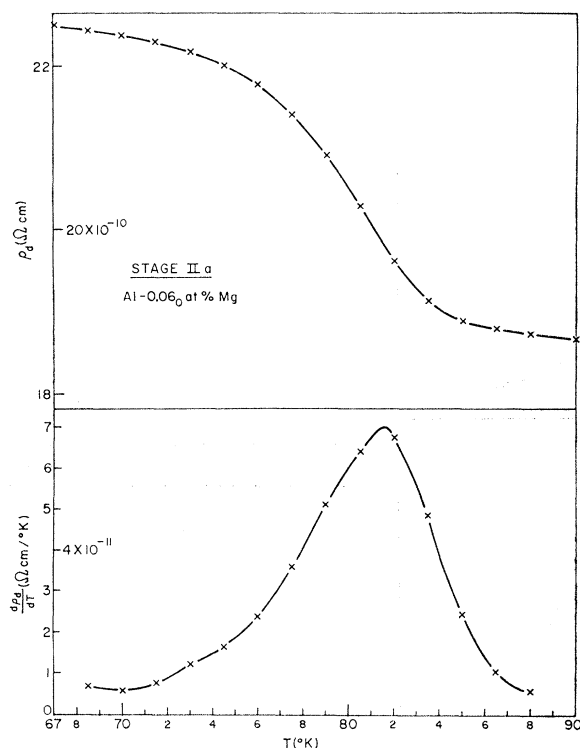


FIG. 4. Isochronal plot of the first substage observed for Al-Mg in the stage-II region, labeled Al-Mg II_A. The lower portion of the figure shows the derivative of the isochronal plot.

In a more recent work, Burger *et al.*²¹ investigated the region between 50 and 150°K in more detail. They report three substages in this region: 71, 83, and about 106°K. The first two peaks show no resolvable temperature shift with defect concentration in their report, but the work was restricted to isochronal studies with varying temperature intervals, typically 5–10°K apart. They no longer attribute the recovery in this region to free interstitial migration.

Wenzl *et al.*²² have investigated the recovery of Al following neutron irradiation by means of residual electrical resistivity, stored energy release, and length changes. From their data they suggest that the recovery in stages I and II is due to close pair annihilation. The results of paper I,²³ based on stage-I recovery, do not support this suggestion. Furthermore, the complex orders of reaction observed in the alloy recovery substages also appear to be in contradiction to this suggestion. One would expect that the trapping by impurities of interstitials who are members of close interstitial-vacancy pairs would lead to a new spectrum of recovery stages, each characterized by first-order

kinetics. Complex orders might only be expected if the interstitial trapping removes the correlation between interstitial and vacancy. However, in such a case migration would occur at or above the stage due to free migration (i.e., above stage II).

Federighi *et al.*²⁴ have presented a different model for the recovery in this region based on the compilation of results of electron and neutron irradiation, deformation, and quenching studies done by many investigators. Their model accounted for the apparent discrepancies (to be discussed later) between the alloy investigations of Ceresara *et al.*,⁹ and Sosin and Rachal,² and the discrepancies in the stage-II_A (60–100°K) region between neutron irradiation studies in which recovery was observed in this region^{20–22} and an electron irradiation study in which recovery was not observed.² The model assigns migration of one type of interstitial (the crowdion) in stage I and migration of a second type of interstitial (the normal) in stage II_A (60–95°K). The rest of stage II is assigned to release from impurity traps. This model is discussed further below.

Most of the above-mentioned results appear to indicate that the region between 60–100°K is solely of an intrinsic nature, supporting in part the present results. However, the results of Snead and Shearin⁵ appear to lead to a different conclusion. Specifically, they reported one substage in this region in their (nominally) high-purity sample (at 78°K). Also they found a similar peak in Al+0.3-at.% Ge (at 83°K), two peaks in Al+0.3-at.% Zn (at 75 and 97°K), and none in the Al+0.3-at.% Cu. From these results it would appear that the peak structure in this region is impurity-dependent and the conclusion reached above, that one peak is intrinsic, would appear to be suspect. Looking closely at the data of Snead and Shearin, one observes that the amounts of recovery in their high-purity sample and the Al-Zn alloy (the first peak, centered at 75°K) are about equal, which may indicate that the recovery is due to the same process as in the base material and not due to the addition of the Zn atoms. Unfortunately, the same does not appear to hold for the Al-Ge alloy.

From the above discussions, the nature of stage II_A cannot be definitely established as yet. Impurities appear to play some role: Al-Mg, Al-Ge, and possibly Al-Zn exhibit substages in this region. Whether or not the impurities are responsible for all the observed recovery in stage II_A is not clear.

C. Stage II-Alloy Substages

Turning more directly now to the behavior of alloy systems, we summarize the results of several investigators in Table III. Of the nine Al-alloy systems studied, three (Al-Si, Al-Mn, and Al-Sn) have not been

²¹ G. Burger, K. Isebeck, H. Meissner, W. Schilling, and H. Wenzl, *Phys. Letters* **20**, 124 (1966).

²² H. Wenzl, W. Schilling, and K. Isebeck, in *Proceedings of the International Conference on Electron Diffraction and Crystal Defects* (Australian Academy of Science, 1965), p. II B-6.

²³ A. Sosin and K. R. Garr, *Phys. Rev.* **161**, 664 (1967).

²⁴ T. Federighi, S. Ceresara, and F. Pieragostini, *Phil. Mag.* **12**, 1093 (1965).

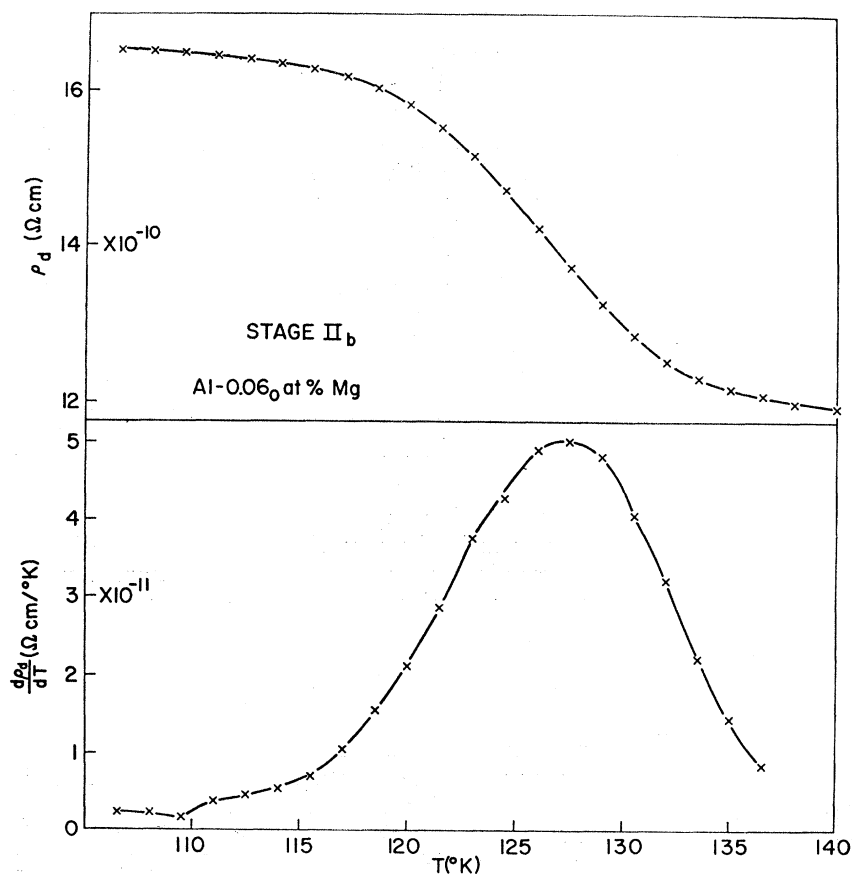


FIG. 5. Isochronal plot of the second substage observed for Al-Mg in the stage-II region, labeled Al-Mg II_b. The lower portion of the figure shows the derivative of the isochronal plot.

investigated below liquid-nitrogen temperature. There is disagreement on the number of substages in stage II for Mg, Zn, Ag, and Sn.

Before attempting to generalize the behavior of the alloy systems, it is worth looking more carefully at the discrepancies in the reported results. Ceresara *et al.* investigated the recovery of several Al alloys following neutron irradiation at liquid-nitrogen temperature. Their procedure included several days delay between the irradiation and the recovery study to allow for

decay of radioactivity. As a result, they failed to observe the lower-temperature (81°K) substage in the Al-Mg alloy system. This particular case points up a need for lower-temperature studies in alloys.

Al-Zn has been, along with Al-Cu, the most widely

TABLE III. Summary of substages in stage II in Al alloys.

Dopant	Number of reported substages in stage II	Reference
Mg	1	9
	2	Present work
Si	1	9
Mn	0	9
Cu	0	2, 5, 9
Zn	1	2
	2	9
	3	5
Ga	2	Present work
Ge	2	5
Ag	0	Present work
	1	9
Sn	0	9
	1	10

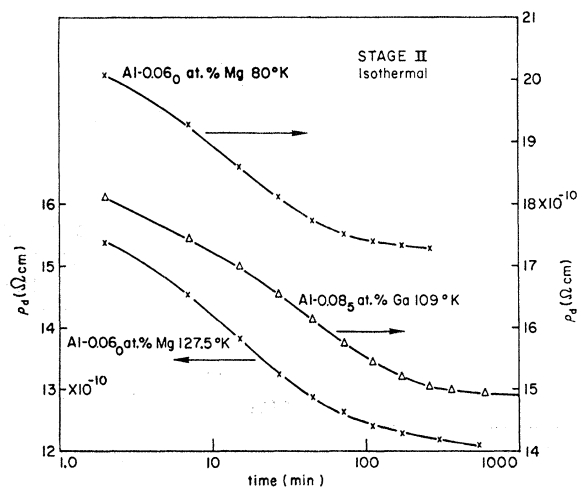


FIG. 6. Isothermal annealing curves for the various substages in the stage-II region. The sample and the isothermal temperature are denoted by each curve.

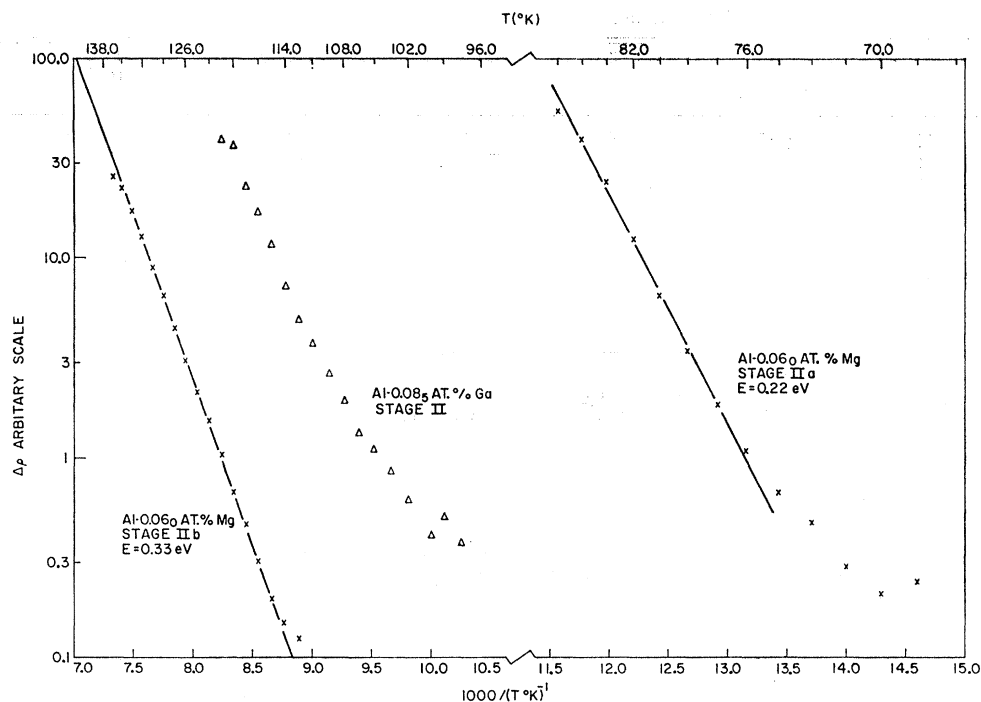


FIG. 7. Determination of the activation energies for the various substages in the stage-II region using the $1/\Delta\rho$ method. The sample and the substage are denoted by each curve. Note the break in the abscissa scales.

investigated alloy. Sosin and Rachal² first reported a single stage of recovery in the stage-II region, centered at about 133°K. Ceresara *et al.* shortly thereafter reported two stages, centered at about 110 and 138°K, respectively (taken from Fig. 1, Ref. 9). Snead and Shearin⁵ recently reported three stages, centered at 75, 97, and 126°K, respectively. In an isochronal investigation, using liquid hydrogen ($\sim 20^\circ\text{K}$) as a coolant, we observed stages centered at 105 and 143°K and a small amount of recovery in the 70–90°K range.

Assuming that the recovery observed in the Al-Zn sample in the temperature range of 70–90°K is characteristic of nominally pure Al (the amount of recovery in this range was the same in the pure Al and Al-Zn samples used, both in Snead's work and the present work) and does not depend on the presence of Zn, it is possible to assign two substages to Al-Zn. The discrepancy with Sosin and Rachal's work² may be explained by noting that their detailed investigation did not start at a low enough temperature to observe the first substage.

The disagreement in the cases of the Al-Ag and Al-Sn alloys cannot be explained as easily as those of Al-Mg and Al-Zn. In the present study no distinct substage was observed in the Al-Ag alloy in the stage-II temperature region which could be attributed to the addition of this solute. In the work of Ceresara *et al.*,⁹ a well-defined substage was reported for the Al-Ag alloy while no distinct substage was reported for the Al-Sn system. However, in a later work on the Al-Sn

system, Ceresara *et al.*¹⁰ reported a substage centered at 138°K.

Federighi *et al.*²⁴ have explained the above-mentioned disagreements in Al-Zn and Al-Ag by postulating, within their model mentioned previously, that neutron irradiation produces both crowdions and normal interstitials, whereas electron irradiation produces only normal interstitials. The discrepancies in the results of Al-Zn and Al-Ag are then explained by arguing that the additional substages observed following neutron irradiation, and not electron irradiation, are due to crowdions produced only by the neutron irradiation. In the same manner, they explained the apparent lack of observation of stage II_A following electron irradiation. (Stage II_A is observed following neutron irradiation.)

This model for the recovery in stages I and II may be criticized in light of more recent experimental evidence. Specifically, stage II_A is observed following electron irradiation (see Fig. 3 and the work of Snead and Shearin).⁵ Also, Snead and Shearin observed more than one substage in the stage-II region for the Al-Zn system, as did the present experimental investigation, and the discrepancy in the alloy results can be explained in a more direct manner as presented earlier.

In attempting to correlate the observation in the several Al alloy systems, some *ad hoc* rules are required because of the discrepancies noted above. We assume, based on the above discussion but with admitted arbitrariness, that there are no substages in stage II for Cu- or Ag-doped Al. We further assume that there

TABLE IV. Substages in stage II and basic properties of alloying elements.

Element	Substages in stage II	Valence	Seitz radii ^a (Å)	Volume ^a size-factor (Å)	Atomic radii ^{b,c} (Å)	Ionic radii ^e (Å)	Electro-negativity ^d
Al	...	2.5 ^e	1.582	...	1.43	0.51(+3)	1.5
Cu	0	1	1.413	-33.77	1.28	0.96	1.9
Ag	0	1	1.598	+ 0.12	1.44	1.26	1.9
Mg	2	2	2.853	+40.82	1.60	0.66	1.2
Zn	2	2	1.538	- 5.74	1.33	0.74	1.6
Ga	2	3	1.672	+ 4.94	1.22	0.62	1.6
Ge	2	4	1.755	+13.13	1.23	0.53	1.8
Si	(1)	4	1.669	-15.78	1.18	0.42	1.8
Mn	(0)	2	1.428	-46.81	1.12-1.49	0.80	1.5
Sn	(0,1)	4	1.862	+24.09	1.40	0.71	1.8

^a H. W. King, *J. Mat. Sci.* 1, 79 (1966).

^b Taken as one half of the elemental bond length.

^c *Handbook of Chemistry and Physics*, edited by Charles D. Hodgman *et al.* (Chemical Rubber Publishing Company, Cleveland, Ohio, 1966), 47th ed.

^d L. Pauling, *Nature of the Chemical Bond* (Cornell University Press, Ithaca, New York, 1960), 3rd ed., p. 93.

^e As determined by Robinson and Dorn (see Ref. 14).

are two substages in the cases of Al (Mg, Zn, Ga, Ge). We feel that it is likely that this rule of either zero or two substages may be quite general, but pending further investigation at lower temperatures, we omit Al (Si, Mn, Sn) from direct consideration for the moment.

Table IV summarizes the situation for the various alloys which have been investigated and gives some atomic parameters which may be appropriate for consideration in any attempt at correlating these observations. [The Seitz radius is defined by $r = (3V/4\pi)^{1/3}$, where V is the atomic volume. The volume size factor

represents the relative difference between the effective atomic volume of the solute and the atomic volume of the solvent.] A study of this table appears to indicate that, in aluminum, the atomic radius is not good, as a single parameter, to correlate with the most elementary annealing result—the number of substages in stage II. Since the Seitz radius and the volume size factor are found to be more useful parameters in the theory of alloys,²⁵ it is possible that they might be more useful here as well. However, the correlation is no better than in the case of the atomic radius. This result is significant

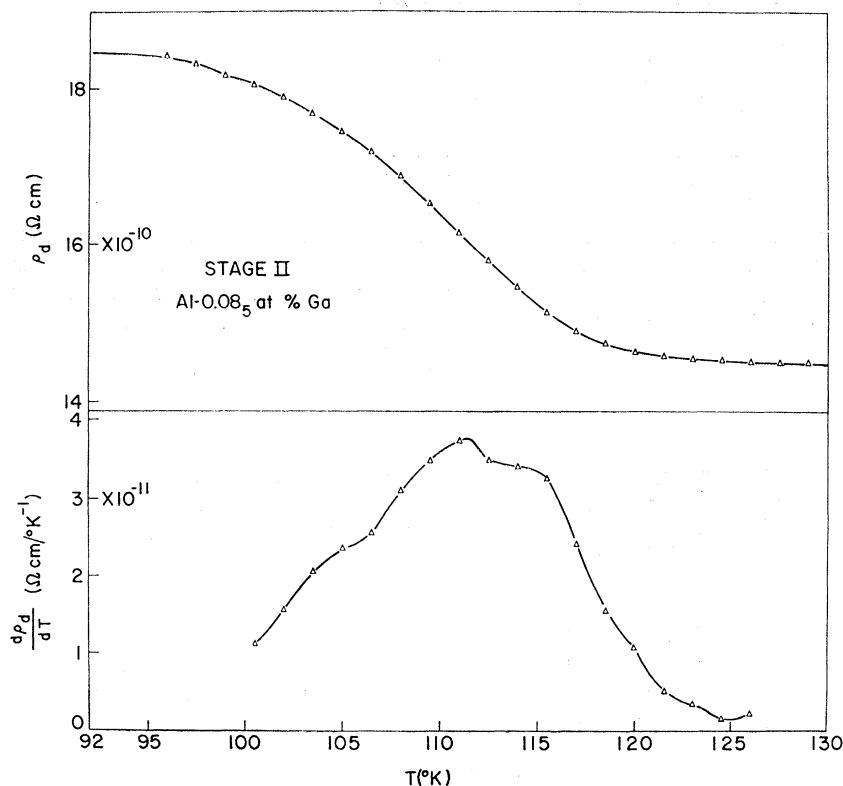


FIG. 8. Isochronal plot of the substage for Al-Ga in the stage II region. The lower portion of the figure shows the derivative of the isochronal plot.

²⁵ H. W. King, *J. Mat. Sci.* 1, 79 (1966).

since many discussions²⁶⁻²⁸ of impurity-point defect interaction are based upon consideration of atomic radius, and atomic size factors have been useful in correlating observations in irradiated copper alloys.^{27,28} Evidently, the relative openness of the aluminum lattice makes size considerations less important: "electronic effects" may be more important in aluminum alloys than "size effects." This seems to be borne out by Table IV. For example, ionic radius is to be preferred as a single parameter over atomic radius, etc., in that the solutes (Mg, Zn, Ga, Ge) which give rise to two substages in stage II all possess smaller ionic radii than solute atoms which we believe give rise to no substages. The possible importance of electronic effects may also be demonstrated upon consideration of electronegativity. Clearly, further experimental work is needed to test whether correlations of this sort are appropriate. In fact, not only the number of substages must finally be considered, but also the values of binding energy should eventually be even more important. Here theoretical assistance is in order.

D. Recovery Kinetics

We now turn to the problem of accounting for the observed values of activation energies, orders of reaction, and vibrational frequencies. An important step in such an accounting is to recognize that the kinetic equation [Eq. (1)] used as a basis for analysis is incorrect in at least two respects. First, diffusional aspects of the problem—spatial dependences—have been neglected. Since the observations reported in paper I²³ demonstrate that considerable migration occurs before stage II, we are led to expect that a fair amount of defect concentration homogenization has been effected, reducing spatial correlations to a minor consideration.

A second limitation to a kinetic reaction formulation leading to Eq. (1) arises from the fact that the reactions in stage II particularly, probably involve at least three reactants so that a set of reaction equations, not a single one, is in order. With due consideration for the limited accuracy of the present data, such effects may be brought into a single reaction equation as follows:

$$dn/dt = -njP_s, \quad (7)$$

where n is the interstitial concentration, j is the number of jumps per second of the interstitial, and P_s is the probability of encountering a sink or "deep" trap in any given jump, resulting in annihilation or complete immobilization.

The number of jumps per second is weighted by the possibilities that an interstitial jumps from a lattice

position well removed from a trapping site or from a "shallow" trapping position. Thus,

$$j^{-1} = (1-c)\nu_f^{-1} + c\nu_b^{-1}, \quad (8)$$

where ν_f is the free jump frequency and ν_b is the frequency of jumps from shallow bound sites. The quantity c is the concentration of shallow traps equal to the concentration of responsible trapping agents multiplied by an appropriate numerical factor to account for an effective trapping radius. Correlation effects are ignored. Further, introducing the binding energy B at shallow traps,

$$\nu_b = \nu_f \exp(-B/kT), \quad (9)$$

so that

$$j = \nu_f [(1-c) + ce^{B/kT}]^{-1}. \quad (10)$$

The probability of encountering a sink or trap on any particular jump is determined by the spatial distributions of such sinks or traps. In the chemical reaction theory approach we take P_s as a function of n . Then

$$\begin{aligned} dn/dt &= \{-\nu_0 e^{-M/kT} / [(1-c) + ce^{B/kT}] f(n) \\ &= -\nu_e e^{-E_e/kT} f(n), \end{aligned} \quad (11)$$

where we have taken $\nu_f = \nu_0 \exp(-M/kT)$; M is the migration energy, and ν_0 is the atomic vibrational frequency. We have introduced an effective vibrational frequency ν_e and an effective activation energy E_e which we identify with the measured quantities. Equation (11) involves two unknowns, ν_e and E_e . To proceed, we note that activation energies are generally derived as the slope of a plot of logarithm of some quantity versus $1/kT$. Thus by first taking logarithms in Eq. (11) and then differentiating with respect to $1/kT$, we obtain

$$E_e = \{ce^{B/kT} / [(1-c) + ce^{B/kT}]\} B, \quad (12)$$

and

$$\begin{aligned} \ln \nu_e &= \ln \nu_0 - \ln [(1-c) + ce^{B/kT}] \\ &+ \{ce^{B/kT} B / kT / [(1-c) + ce^{B/kT}]\}. \end{aligned} \quad (13)$$

With this formulation, it is possible to appreciate the origin of some of the kinetic parameters which emerge in this study. Some typical results are given in Fig. 9, where we have examined the effects on the effective frequencies and energies for two cases in which $M=0.11$ eV, $B=0.11$ and 0.22 eV, and $T=81$ and 127°K , respectively. These parameters correspond to the two annealing substages observed in the Al-Mg alloy assuming that the free migration energy of an interstitial is 0.11 eV. In both cases, the effect of the trap density on E_e is rather clear and indicates that, with the impurity concentrations used experimentally, $E_e = M + B$. Note that at lower concentrations intermediate values, between M and $M+B$, may apply. However, for the parameters used above, the purity of the material needed to observe these lower values of E_e are about an order of magnitude lower than the

²⁶ J. D. Eshelby, *Acta Met.* 3, 487 (1955).

²⁷ R. R. Hasiguti, *J. Phys. Soc. Japan* 15, 1807 (1960).

²⁸ A. Sosin, *Lattice Defects and Their Interactions*, edited by R. R. Hasiguti (Gordon and Breach Science Publishers, Inc., New York, 1967).

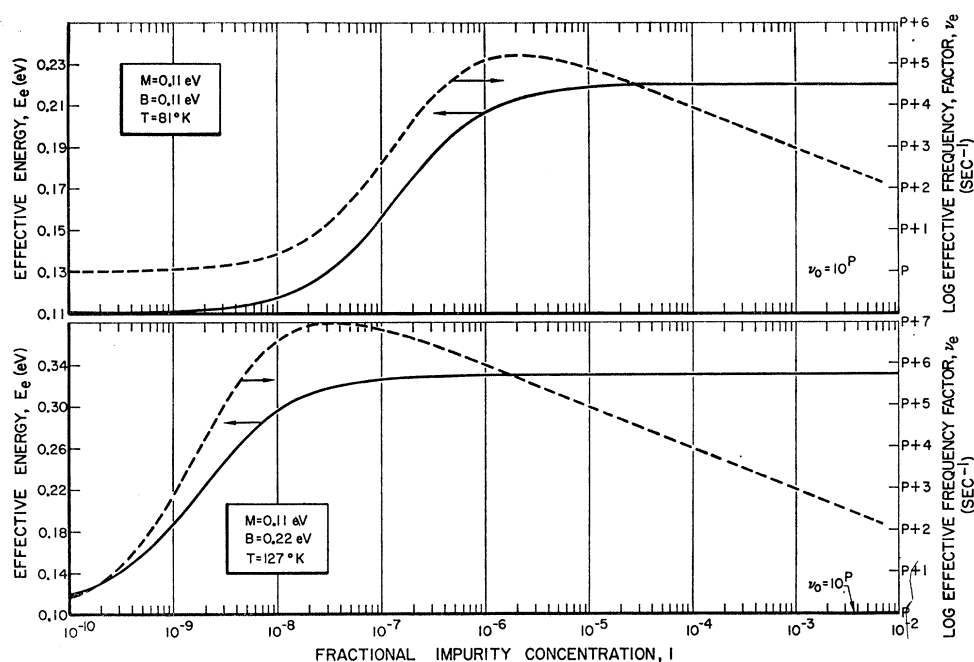


FIG. 9. Case study of effective activation energies and frequency factors. The change in effective energy E_e is simple and monotonic with trap density. The effective frequency goes through a maximum.

purest material used in the present study. In paper III,¹² examples are cited where the intermediate cases may be applicable.

The effect on the effective frequency factor is more dramatic; the effective frequency may become appreciably greater than the atomic frequency over a wide range of trap density concentrations. The general feature of effective frequency is a rather sharp rise to a maximum followed by a slow linear decrease over several decades of trap concentrations.

The only value of the effective frequency which was determined experimentally with sufficient accuracy for discussion was for the Al-Mg II_A substage (see Table II). Comparing the calculated results with the experimental, we see that good agreement is obtained for $\nu_0 \sim 5 \times 10^{12} \text{ sec}^{-1}$.

It is more difficult to account for the apparent order of kinetics observed here. We write, following Nihoul and Stals,¹⁶

$$f(n) = -K_1 n^{\bar{\gamma}}, \quad (14)$$

where $\bar{\gamma}$ is an effective order of reaction. Then

$$\bar{\gamma} = d \ln f(n) / d \ln n \quad (15)$$

or

$$\bar{\gamma} = [n/f(n)] [df(n)/dn]. \quad (16)$$

We now consider a process which is intermediate between first and second order:

$$f(n) = -K_2(n^2 + nI), \quad (17)$$

where I is constant and corresponds to an impurity concentration. Then, in this example,

$$\bar{\gamma} = 1 + (n/n + I). \quad (18)$$

From such an analysis, we would expect that $\bar{\gamma} \approx 1$ in all the alloy studies examined here unless the cross section for impurity-interstitial reaction is unexpectedly small.

Alternative to the above formulation, we might attempt to include spatial distribution considerations. The framework for such an analysis has been laid by Waite²⁹ and further developed recently by Nihoul and Stals.¹⁶ Nihoul and Stals conclude that the Meechan-Brinkman¹⁷ procedure for deducing a value of γ is valid only if γ is constant, which is never the case when spatial distribution effects are taken into account.

We have used Eq. (16) in data analysis and have found little change in the derived values of $\bar{\gamma}$; a slight decrease $\lesssim 0.2$ might be justified. The analysis performed by Nihoul and Stals, à la Waite, does not fit our data nor would it be expected to do so since our distribution in stage II is distinctly nonrandom. The Waite formulation can be extended to distributions which we believe correspond to stage II, but we have not yet attempted this.

It appears that both experimental data with greater resolution and accuracy and more applicable analytical formulation are needed before the details of stage-II annealing can be made definitive. However, one important conclusion regarding kinetics can be made and stressed: The annealing in stage II in the present alloys does not follow simple first-order kinetics. The deviation from first order implies a degree of random interstitial diffusion.

²⁹ T. R. Waite, Phys. Rev. **107**, 463 (1957); **107**, 471 (1957).

V. SUMMARY

The addition of foreign atoms into nominally pure Al produces changes in the recovery of the residual electrical resistivity following low-temperature irradiation with either electrons or neutrons. These changes, in conjunction with the observations of other experiments, have given some indication as to the nature of the interaction of solute atoms with interstitials.

The addition of solute atoms in pure Al causes a suppression of the recovery normally observed in the pure material. This suppression is about 20–27% of the recovery observed in the pure material and appears to take place mainly in a temperature region above 35°K.

Stage II_A (60–100°K) is a region in which defect identification is uncertain. Some evidence leads to the conclusion that an intrinsic defect migrates in this region while other data appear to indicate that impurity detrapping is the prominent process. The bulk of stage II, however, is rather clearly due to the release of interstitials, trapped during migration in stage I, from impurity-trapping sites. Based on the number of

substages observed for different solute atom additions by several investigators, it appears that, in Al, “electronic effects” are more important in determining the strength of the solute atom interstitial interaction than are “size effects” and that the ionic radius may be a reasonably valuable factor to use when correlating the interaction to some atomic parameter. However, there are still some unresolved discrepancies in the results of different investigators, and more work will be needed in order to justify the above generalities.

High effective frequency factors and varying measured energies may be accounted for with an impurity-trapping model. Thus the energies measured represent the sum of the actual migration energy of interstitials plus some fraction of a binding energy of interstitials to an impurity or impurity-interstitial cluster. The fractional order of reaction which was observed is understood to indicate a complex annealing process.

ACKNOWLEDGMENTS

We gratefully acknowledge the comments and suggestions made by W. Bauer and K. Thommen.

Recovery of Electron-Irradiated Aluminum and Aluminum Alloys. III. Stage III

K. R. GARR*

Atomics International, Division of North American Aviation, Incorporated, Canoga Park, California

AND

A. SOSIN

North American Aviation Science Center, Thousand Oaks, California

(Received 22 May 1967)

The recovery of the residual electrical resistivities of pure Al and the Al alloys (nominally 0.1 at.%) Al-Mg, Al-Ga, and Al-Ag have been investigated following 1-MeV electron irradiation near 4°K. Analysis of the data for nominally pure Al in stage III (170–300°K) discloses substructure. (A very small substage occurs at lower temperatures and appears to be influenced by the residual impurities.) The main portion of the stage shows a variation in the observed activation energy with purity: The higher the purity of the “as-received” material, the lower the observed activation energy. A range of 0.46 to 0.59 eV was found for the materials investigated. The effective frequency factor for these materials showed a concurrent systematic variation. These effects are believed to be due to the interaction of migrating defects with residual impurities in the material. The recovery of the alloys in the stage-III region is more complex than in the pure material. There is more substructure in the recovery spectrum of the alloys, and the observed activation energies in stage III are higher. Al-Ag showed a resistivity decrease followed by an increase which is attributed to the clustering of Ag atoms. The observations are interpreted in terms of interstitial migration, restricted by impurities, in the earlier portion of stage III; vacancy migration becomes important in the latter portion of stage III. Stated differently, interstitials migrate in stage III and vacancies migrate in stage IV, but in Al these stages overlap appreciably.

I. INTRODUCTION

THE role of impurities in stage-III recovery in metals remains unclear, and some apparently contradictory results are present in the literature,^{1–8}

despite rather extensive investigation. At one extreme, the study of Sosin and Rachal³ of the recovery of

* Work supported by Division of Research, Metallurgy, and Materials Programs, U. S. Atomic Energy Commission, under Contract No. AT(04-3)-701.

¹T. H. Blewitt, R. R. Coltman, C. E. Klabunde, and T. S. Noggle, *J. Appl. Phys.* **28**, 639 (1957).

²D. G. Martin, *Phil. Mag.* **6**, 839 (1961); **7**, 803 (1962).

³A. Sosin and L. H. Rachal, *Phys. Rev.* **130**, 2238 (1963).

⁴S. Ceresara, T. Federighi, and F. Pieragostini, *Phys. Letters* **6**, 152 (1963).

⁵S. Ceresara, T. Federighi, and F. Pieragostini, *Phil. Mag.* **10**, 893 (1964).

⁶C. L. Snead and P. E. Shearin, *Phys. Rev.* **140**, A1781 (1965).

⁷F. Dworschak and J. S. Koehler, *Phys. Rev.* **140**, A941 (1965).

⁸D. A. Grenning and J. S. Koehler, *Phys. Rev.* **144**, 439 (1966).